ELSEVIER

Journal of Nuclear Materials 283–287 (2000) 234–238

journal of nuclear materials

www.elsevier.nl/locate/jnucmat

Study of point defect behaviors in vanadium and its alloys by using HVEM

T. Hayashi *, K. Fukumoto, H. Matsui

Institute for Materials Research, Tohoku University, Katahira 2-1-1, Aoba-ku, Sendai 980-8577, Japan

Abstract

Microstructural evolution and point defect behavior in vanadium and V–xFe ($x = 0.1$, 0.2, 0.3, 3, 5 at.%) have been examined by using high voltage electron microscopy. During irradiation, interstitial-type dislocation loops are formed and grow in all materials. In V–xFe, measured saturated loop number density is much higher than that in pure vanadium, indicating iron atoms in the matrix strongly interact and trap self-interstitial atoms (SIAs). The shapes of loops formed in V–xFe are complicated, i.e., loops grown to >100 nm show stacking fault-like shapes. Those complicated shapes become more significant with increasing iron concentration. This means iron atoms segregate to loops through the strong interaction with SIAs. The apparent migration energies of 0.21 eV and 0.81 eV have been determined from the temperature dependence of loop number density for pure vanadium and V–xFe, respectively. Various observed phenomena are discussed in terms of the obtained binding energy.

1. Introduction

Vanadium-base alloys are considered as candidate structural materials for fusion reactors because of their attractive properties such as low radiation-induced activation, high thermal conductivity, low thermal expansion and superior resistance against swelling [1,2]. However, the behavior of point defects in vanadium and its alloys has not been clarified enough. In order to evaluate material performance after severe, and often non-steady irradiation conditions, fundamental parameters of point defects, e.g. migration energy of point defects, are essential.

On the other hand, it is known that vanadium alloys containing undersized solute atoms exhibit unexpectedly large amount of swelling after neutron irradiation [3,4]. It is also important to understand the mechanism of such strong swelling enhancement by undersized solute atoms, e.g. iron.

A number of HVEM experiments have been conducted on pure metals and alloys [5–7], including vanadium alloys [8], and have lead to substantial understanding of point defect behavior, i.e., their mobility and interactions with impurity atoms and solute atoms through in situ observation of microstructural evolution. However, the HVEM experiments on vanadium alloys have been obstructed by surface contamination and bending of the thin foil specimens caused by environmental impurities at high temperatures. In this study, to avoid such specimen degradation and obtain the reliable parameters, we conducted the experiments using a relatively high vacuum HVEM ($\sim 10^{-6}$ Pa), and at low temperatures where degradation does not occur.

2. Experimental procedure

Pure vanadium of 99.9% purity and V–xFe ($x = 0.1$, 0.2, 0.3, 5) were used in this experiment. These V–xFe alloys have been selected in order to examine the point defects behavior in a wide range of Fe concentration. The ingots of V–xFe alloys were cold rolled to approximately 0.2 mm thick sheets. TEM disks with diameter of 3 mm were punched from sheet specimens followed by electro-polishing. The recrystallization

* Corresponding author. Tel.: +81-22 215 2069; fax: +81-22 215 2066.

E-mail address: hayashi@fusion.imr.tohoku.ac.jp (T. Hayashi).

0022-3115/00/$ - see front matter
PII: S0022-3115(00)00104-5

annealing was done at 1327 K in a vacuum of 2×10^{-4} Pa for 2 h. The disks were thinned by electropolishing for TEM observation.

Electron irradiation and in situ microstructural observations were conducted in the HVEM (JEM ARM-1250) in the High Voltage Electron Microscope Laboratory at Tohoku University at an electron acceleration voltage of 1250 kV. The irradiation temperature and damage rate ranged from RT to 523 K and from 7.1×10^{24} to 3.6×10^{25} e/m^2 s, respectively.

3. Results

3.1. Microstructure evolution during irradiation in pure V and V–0.1Fe

Fig. 1 shows the typical microstructural changes in pure V (a) and V–0.1Fe (b) during irradiation at 493 K. Interstitial-type dislocation loops are formed and grow in all the irradiation conditions and materials. The loop number density initially increases with irradiation dose, and soon saturates. Saturated loop number density is higher at lower temperature and for higher beam intensity, and loops grow more rapidly at higher temperature and higher intensity. In pure V, loops grow very fast at high temperatures to tangle with each other and some of loops glide to foil surface and disappear during irradiation. In V–xFe, glide of loops is hardly observed even at high temperatures. Loop density is much higher and loop growth rate is much lower in V–xFe than those in pure V. It follows that adding Fe atoms increases loop nucleation, but reduces loop growth rate. These observed phenomena suggest Fe atoms in the matrix strongly interact and trap self-interstitial atoms (SIAs), and as a result, segregate to SIA-type loops.

3.2. Microstructure evolution during irradiation of V–xFe

Examples of loop evolution in V–0.1Fe, V–0.3Fe and V–5Fe at 473 K are shown in Fig. 2. At lower dose, loop nucleation and growth are observed in a same manner in all V–xFe alloys and pure V. In a series of V–xFe alloys, unexpectedly, loop number density did not increase monotonically with increasing iron concentration; loop number density in V–0.1Fe is higher than other V–xFe alloys with higher Fe concentration. As seen in the micrographs, loop growth rate in V–0.1Fe is more rapid than other V–xFe alloys, and the loop growth rate decreased with increasing iron concentration.

Moreover, at higher doses, loops in V–xFe alloys show gradually complicated shapes as they grow larger. The complicated shapes become more significant with increasing iron concentration. Fig. 3 shows loop evolution at 523 K in V–5Fe. Loops with small black dot contrast at low dose (Fig. 3(a)) grow to have a flower-like shape with a diameter of about 100 nm, as shown in Fig. 3(b). These flower-like loops grow to a diameter greater than 100 nm and acquire stacking fault-like fringe contrast and their peripheral dislocations show dotted contrast (Fig. 3(c)). Dislocation loops with fringe contrast have been observed in other neutron and/or

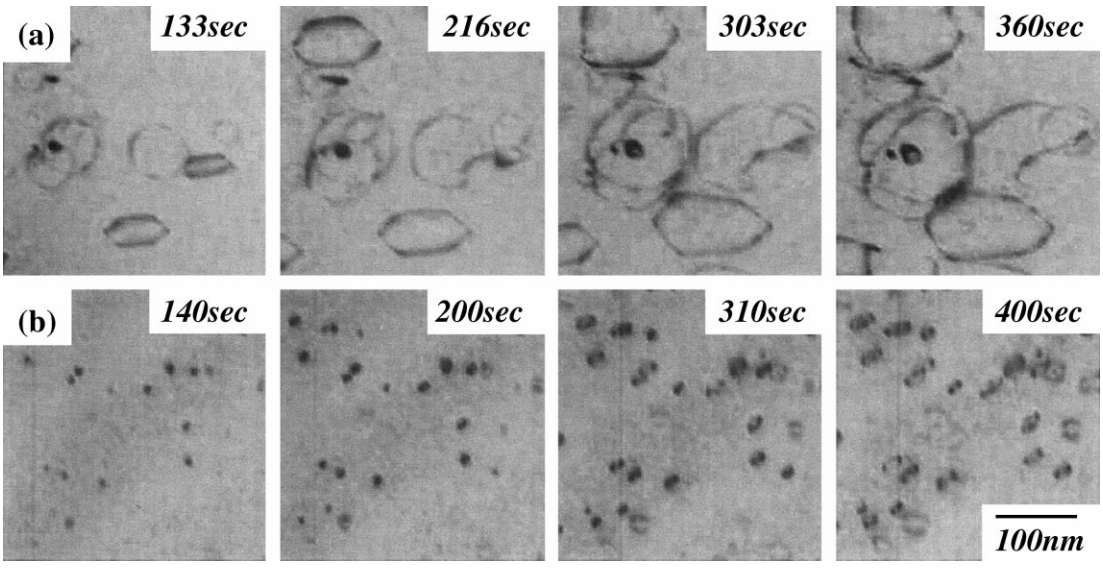

Fig. 1. Typical microstructural evolution in pure V (a) and V–0.1Fe (b) during irradiation at temperature of 493 K and beam intensity of 2.1×10^{25} e/m^2 s.

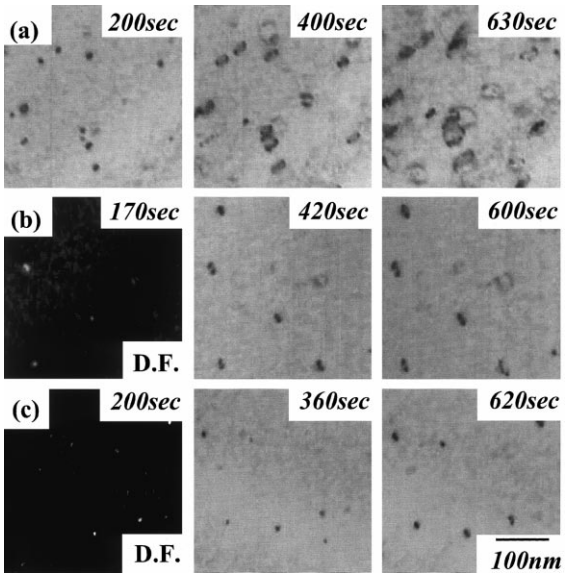

Fig. 2. Typical microstructural evolution in V–0.1Fe (a), V–0.3Fe (b) and V–5Fe (c) during irradiation at temperature of 493 K and beam intensity of 2.1×10^{25} e/m^2 s. Photographs labeled D.F. are dark field images.

heavy ion irradiation experiments on V–5Fe. A similar contrast would be observed if there are thin layers of another phase present. Since the formation energy of a stacking fault in bcc vanadium alloys is very high, loops with fringe contrast observed in this study are considered to be caused by a thin layer with a different chemical composition, formed by segregation of iron atoms to the loops.

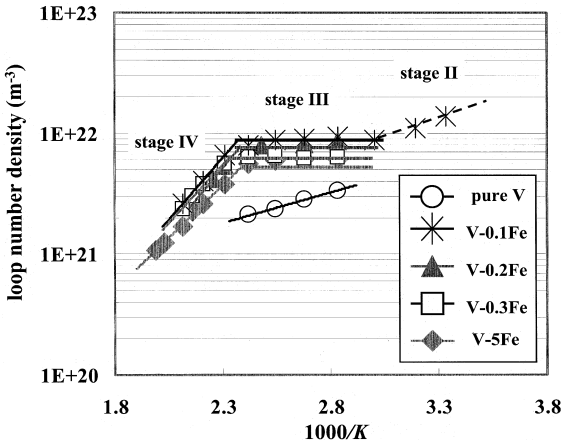

Fig. 4. Arrhenius plot of loop number density in pure V and V–xFe.

4. Discussion

4.1. Analysis of measured loop number density

Fig. 4 shows the Arrhenius-type plot of measured loop number density. From this figure, there are three temperature stages, i.e., two stages showing linear inverse temperature ($1/T$) dependence, labeled stage II and IV, and a temperature independent stage, labeled stage III. In order to analyze the data obtained from HVEM experiments, rate theory equations for loop nucleation assuming that di-interstitials are stable loop nuclei, proposed by Yoshida et al. [5], have been used. According to this study, these stages in Fig. 4 appear when the interactions between SIA and impurities become

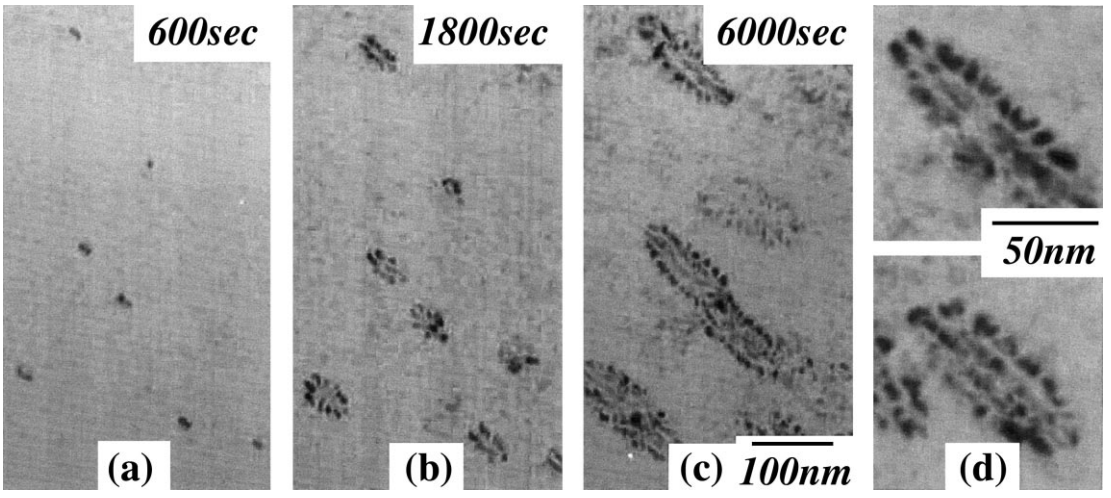

Fig. 3. Dislocation loop evolution in V–5Fe during irradiation at 523 K. (a) low dose (600 s); (b) higher dose (1800 s); (c) highest dose (6000 s) and (d) high magnification image of larger loops formed after irradiation to high dose (6300 s).

strong and dominate loop nucleation, and have been understood as follows:

1. Stage III: Impurities trap SIAs strongly to provide loop nucleation sites. The saturated loop number density shows no dependence on both irradiation temperature and beam intensity, and should correspond to the impurity concentration in the matrix.
2. Stage IV: Trapping and detrapping by impurities take place and loop number density have linear $1/T$ dependence on irradiation temperature and square root dependence on beam intensity.

Fig. 5 shows the beam intensity dependence of loop number density at various temperatures corresponding to each stage. The results shown in Fig. 5 are in good agreement with the consequences from the above-mentioned analysis based on rate theory, confirming di-interstitials are stable loop nuclei both in pure V and V–xFe alloys. Since the loop density in stage II was too high to measure exactly, and the data in this stage II are not sufficient, it was difficult to extract more information on the process dominating this stage.

4.2. Migration energy of SIA

In the case where di-interstitials act as stable nuclei, as confirmed in the previous section, the apparent migration energy of SIA have been estimated from the slopes of lines in Fig. 4 using rate theory equations. The obtained values of apparent migration energies are 0.21 eV in pure V and 0.81 eV in V–xFe, respectively. In the case of V–xFe alloys, the apparent migration energy obtained from the slope in stage IV represents the sum of migration energy of SIAs and binding energy between SIA and impurity atom (or iron atom). Based on this argument, binding energy of 0.6 eV has been obtained.

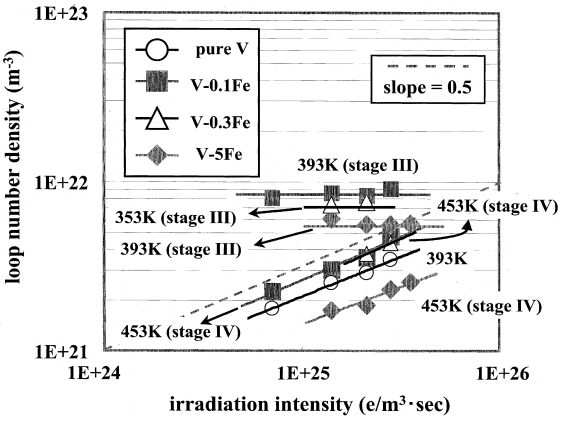

Fig. 5. Dependence of loop number density on irradiation intensity in pure V and V–xFe at various temperatures corresponding to each temperature stage.

Here, the results in Fig. 4 and parameters obtained above indicate, in V–xFe, impurities and/or iron atoms strongly trap SIAs during irradiation and provide loop nucleation sites, leading to the appearance of three temperature stages. As already mentioned above, the loop number density in stage III should correspond to the concentration of impurity atoms responsible for loop nucleation. It is likely that iron atoms are acting as nucleation centers for SIAs since iron is an undersized solute atom and is considered to have strong binding with SIAs. In the present experiments, however, the loop number density in stage III gradually decrease with increasing iron concentration. Thus, it is difficult to consider iron atoms, or at least single iron atoms, are acting as loop nucleation sites. It follows that impurities are playing a major role in effective loop nuclei in V–xFe.

However, a question still remains in this case. That is, if iron atoms do not contribute to form loop nuclei at all, and the same kind of impurity, e.g. oxygen, acts as loop nucleation sites both in pure V and V–xFe, the stage III should appear also in pure V. This is apparently not the case in this study.

One possible mechanism causing these phenomena lies in a formation of mobile V–Fe mixed and Fe–Fe pure dumbbells with a lower mobility than V–V pure dumbbells in V–xFe alloys. Loop nucleation takes place through migration of these mixed dumbbell interstitial atoms to impurity sites. If impurities trap V–Fe and Fe–Fe dumbbells more strongly than V–V pure dumbbells, it is probable that stage III appears in V–xFe alloys, but not in pure V, and loop number density at stage III may decrease with increasing iron concentration. Of course, some questions still remain in this consideration, i.e., V–Fe and Fe–Fe dumbbells are trapped by impurity atoms in the matrix more strongly than V–V pure dumbbells. Another possible mechanism is that loop nucleation takes place through migration of three types of dumbbells to form immobile di-interstitials consisting of one or two iron atoms. The fraction of V–Fe mixed and/or Fe–Fe pure dumbbells increase with increasing iron concentration in the matrix. This phenomenon may cause a decrease of the number of loop nuclei with increasing iron concentration. Moreover, a decrease in mobility of interstitial atoms leads to enhance the fraction of recombination. This mechanism also suppresses the loop nucleation. The probability of forming V–Fe and/or Fe–Fe dumbbells, which need higher activation energy for long range migration than V–V pure dumbbells, increases with increasing iron concentration in the matrix. Thus, loop number density in V–5Fe is also lower than other V–xFe alloys with lower iron concentration. However, there also remains some questions in this consideration. Thus, more investigation is needed to understand the complicated phenomena observed in this study.

4.3. Effects of iron atoms on large swelling observed in neutron irradiation experiments

One of the objectives in this study using HVEM on pure V and V–xFe is to obtain further understanding of the mechanism of giant swelling observed previously in neutron irradiation experiments. As mentioned in Section 3.2, loops with fringe contrasts as seen in this study have also been observed in previous neutron experiments as defects with thin solute layers. These thin layers should have important effects on dislocation evolution. That is, large swelling should be accompanied by enhanced dislocation evolution. However, to the contrary, the results obtained in this experiment showed loop growth rate decreased with increasing Fe concentration as shown in Figs. 1 and 2.

One of the possibilities causing this discrepancy lies in the difference of irradiation temperature between this experiment and previous neutron experiments. In this experiment, irradiation was conducted below 573 K to avoid specimen degradation. However, the giant swelling in V–5Fe in neutron experiments are observed above 673 K, and loop growth rates between the two temperature regions separated at about 623 K are significantly different [9,10]. It indicates the possibility that dislocation evolution changes significantly at about 623 K by some unknown mechanisms. One possible mechanism is an increase of mobility of SIA–Fe mixed dumbbells above 623 K. It is likely that V–Fe mixed dumbbells migrate more readily than V–V pure dumbbells to dislocations in the vicinity of them [11]. In the bulk of the crystal, however, the migration energy of mixed dumbbells is considered to be much higher than pure dumbbells. In this case, it follows that dislocation evolution in V–xFe is slower than that in pure V. Indeed, loop growth rate in V–xFe was lower than that in pure V as observed in this study, and the same tendency has been observed in neutron experiments when irradiation was conducted below 623 K [9]. Unfortunately, we could not conduct the experiment above 623 K because of specimen degradation, and the mechanism of the change of dislocation evolution behavior at about 623 K will be one of the future subjects.

5. Conclusion

The microstructural evolution and point defect behavior during irradiation have been studied by using HVEM on pure V and V–xFe alloys with a wide range of iron concentration in order to examine the interaction between SIAs and iron atoms. It is also intended to obtain further understanding of the effects of iron atoms on giant swelling.

SIA-type dislocation loops are formed and grow in all the irradiation conditions and materials. Adding iron atoms resulted in effective increase of loop density and decrease of loop growth rate.

1. Loops with fringe contrasts have been observed in V–xFe alloys after irradiation to high dose, and these defects are considered to be formed due to segregation of iron atoms to loops.
2. There have been three stages in the Arrhenius-type plot of loop number density in V–xFe alloys; two stages showing linear $1/T$ dependence and a temperature independent stage. From the temperature dependence of loop number density, the migration energy of the SIA has been determined to be 0.21 eV and 0.81 eV for pure V and V–xFe alloys, respectively.
3. The results obtained in this study provide no straightforward explanations for the mechanism of giant swelling. However, some considerations based on the results obtained in this study have been proposed.

Acknowledgements

The authors are deeply indebted to E. Aoyagi and Y. Hayasaka in High Voltage Electron Microscope Laboratory in Tohoku University for their technical assistance in using HVEM.

References

[1] B.A. Loomis, A.B. Hull, D.L. Smith, J. Nucl. Mater. 179–181 (1991) 148.
[2] B.A. Loomis, D.L. Smith, J. Nucl. Mater. 191–194 (1992) 84.
[3] H. Matsui, D.S. Gelles, Y. Kohno, Effects of Radiation on Materials, Proceedings of the 15th International Symposium, ASTM-STP 1125 (1992) 928.
[4] H. Matsui, H. Nakajima, S. Yoshida, J. Nucl. Mater. 205 (1993) 452.
[5] N. Yoshida, M. Kiritani, F.E. Fujita, J. Phys. Soc. Jpn 39 (1975) 170.
[6] H. Inoue, T. Muroga, Y. Miyamoto, N. Yoshida, J. Nucl. Mater. 191–194 (1992) 1342.
[7] S. Watanabe, A. Aoki, H. Murakami, T. Muroga, N. Yoshida, J. Nucl. Mater. 155–157 (1988) 815.
[8] T. Muroga, K. Araki, N. Yoshida, ASTM-STP 1047 (1990) 199.
[9] Y. Chandra, K. Fukumoto, H. Matsui, J. Nucl. Mater. 271&272 (1999) 301.
[10] K. Kuji, A. Kimura, H. Matsui, Sci. Rep. RITU A 40 (1994) 121–124.
[11] H. Kamiyama, H. Rafii-Tabar, Y. Kawazoe, H. Matsui, J. Nucl. Mater. 212–215 (1999) 231.